

Analysing outage probability of linear and non-linear RF energy harvesting of cooperative communication networks

ISSN 1751-9675
 Received on 14th January 2020
 Revised 17th July 2020
 Accepted on 3rd August 2020
 doi: 10.1049/iet-spr.2019.0612
 www.ietdl.org

Vu Van Son¹, Dinh Trieu Duong², Tran Manh Hoang³, Do Thanh Quan¹, Pham Thanh Hiep¹ ✉

¹Le Quy Don Technical University, Ha Noi, Vietnam

²University of Engineering and Technology, Ha Noi, Vietnam

³Telecommunication of University, Nha Trang, Vietnam

✉ E-mail: phamthanhiep@gmail.com

Abstract: In this study, a dual-hop cooperative communication system with radio frequency (RF) energy harvesting was investigated in two cases of linear and non-linear energy harvesting models. In the proposed system, the signal is transmitted directly from a source node to a destination node or sent with support of selected relay nodes. While both the source node and the destination node are powered normally, the relay nodes are powered by harvesting technique. To choose the best relay node, a selection combination method was applied at the destination node in both cases of amplify-and-forward and decode-and-forward protocols. To evaluate the system performance, the outage probability of the cooperative communications over independent identically distributed Nakagami- m was derived and analysed with arbitrary m parameter whereas this parameter was fixed to be integral value in previous research studies. Furthermore, the approximate and asymptotic operations are applied to simplify the outage probability expressions. The simulation program was developed based on the Monte Carlo method and MATLAB software with two aims of evaluating the system performance and verifying the theoretical results. The simulation results demonstrate that the analysis and evaluation of the study are considerably accurate.

1 Introduction

There have been many techniques applied to extend the coverage of wireless networks in which cooperative communication appeared as a principal solution. Two relaying protocols, amplify-and-forward (AF) and decode-and-forward (DF) [1, 2], are used mainly in the cooperative networks. At the relay nodes, signals from the source are amplified and then forwarded to the destination in the AF protocol, while they are decoded and then forwarded to the destination in the DF protocol. If there are multiple relay nodes available, a relay selection technique, i.e. partial relay selection or full relay selection [3, 4] is used to determine the best relay node based on channel state information (CSI).

On the other hand, radio frequency (RF) energy transmission and harvesting will be applied as prime alternative approaches to supply electric power in the future wireless networks [5]. Especially, in many wireless networks with energy-constrained support such as wireless sensor networks or wireless body area networks, these techniques may become a fundamental method to provide power for devices to overcome the limited lifetime and small size issues. A number of previous emerging research studies have shown that it is possible to supply the relay nodes by energy harvesting (EH) technique from around radio environment and then a combination of relaying protocol with EH technique has been developed and proposed for many state-of-the-art communication systems, which is carefully reviewed as follows.

In [6], the authors developed and realised the hybrid downlink for both information and energy in the massive multiple-input-multiple-output (MIMO) systems in which the information and energy are simultaneously transmitted to information users and energy users based on finding out the approximate optimal power allocation of the information users. In [7], the authors investigated the cooperative communication system having multiple-antenna transceivers. In the proposed system, data is exchanged with the help of the relay-supported network employing a single-carrier communication scheme and the relay nodes are powered by the harvesting energy method from the surrounding environment to forward received data signals to the destination nodes using the harvest-then-forward scheme.

In addition, based on an assumption that a direct link is not available, to evaluate system performance, Do *et al.* in [8] found out the closed-form expression for the outage probability (OP) of the dual-hop decode-and-forward (DF) relaying communication system in which the time switching (TS)-based relaying mechanism is applied. Moreover, with the purpose of improving the performance of the cooperative communication network utilised the DF protocol and EH relays, authors in [9] studied and proposed a selection approach to determine the best relay node to forward the signal to destinations in which two operation schemes at the relays, the power splitting (PS) and the TS, were analysed. In [10], the EH AF relaying networks were examined under the condition that the channel is affected by interference and the Nakagami- m fading, demonstrating that the TS scheme is more sensitive to EH technique than the PS scheme with the same channel parameters and settings.

Moreover, all previous works mentioned above considered the linear EH model with a fixed energy conversion efficiency. To simplify the analysis, the energy conversion efficiency is assumed to be independent of the input power of the EH circuit and the amount of the harvested energy is linearly proportional to the input power. However, in practice, the EH circuits have a non-linear behaviour and depend on the input power of RF-direct current (DC) circuits [11–13].

In practical designs, an imbalance between output and input often happens because the EH circuits are likely to be non-linear. The non-linear EH circuits applied for dual-hop DF relaying system were investigated in [14, 15]. In these works, the system performance in terms of the OP expression was analysed, demonstrating that the non-linear EH circuit greatly impacts the system performance. Besides, Dong *et al.* [16] illustrated the effect of the non-linear characteristic of the RF EH circuits on the performance of the cooperative communication system having wireless powered relay and utilising AF protocol under an assumption that the channel has the Nakagami- m distribution.

Moreover, there were some relative previous papers of our members about relaying system employing wireless power transfer. For example, Hoang *et al.* [17] focused on Rayleigh fading channels, the relationship between the EH duration and

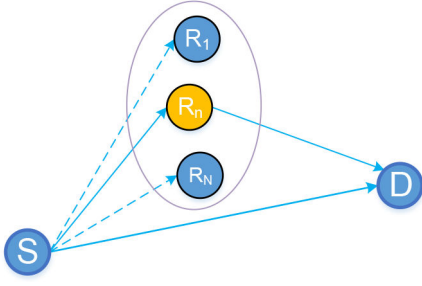


Fig. 1 Wireless power supply cooperative relay selection networks

communication duration in non-orthogonal multiple access (NOMA) relay systems has been analysed [18] and the duration of EH for downlink NOMA full-duplex relay systems were also optimised in [19]. In the conference paper by Hoang *et al.* [20], we started to analyse the performance of the wireless power supply relay networks with the DF protocol based on the OP.

As mentioned above, there have been a number of previous works on the systems utilised a combination of the cooperative communication with wireless power transfer due to its potential benefits and applications. However, there has not been an issue about combining the cooperative communication and RF EH under the condition that the direct link between source and destination exists for such systems with relay selection methods over Nakagami- m fading channels yet. Especially, an analysis based on the arbitrary m parameter has not been taken into consideration as well. As a result, the fundamental target of this paper was to analyse the cooperative communication system employing selected relaying and EH in which there is an existence of the direct link or in other words the source node may communicate with the destination node directly or by the support of the relay nodes, demonstrating that the proposed system model is more practical. Besides, the outage performance of the proposed systems is investigated in two scenarios, i.e. linear and non-linear EH models to provide a practical analysis.

In the linear EH model, the system performance was evaluated through the OP in both cases of AF and DF protocols over Nakagami- m fading channels with the arbitrary m value while only the DF protocol is mentioned in the non-linear EH model.

The rest of the paper is arranged as follows. Section 2 illustrates the system model and analyses the end-to-end signal-to-noise ratio (SNR). Section 3 explains the linear and non-linear EH modes, and then the signal processing of the proposed system is represented in Section 4. Section 5 develops and derives the OP expression for the AF and DF protocols. Section 6 informs theoretical analysis and simulation results. Finally, Section 7 provides the conclusion.

Notation: In the paper, some main notations are used as follows. The binomial coefficient and factorial of (\cdot) are expressed by $\binom{n}{k} = \frac{n!}{k!(n-k)!}$ and $(\cdot)!$, respectively. R_b denotes the best selected relay node. The gamma function [21, Eq. (8.310.1)], upper incomplete gamma function [21, Eq. (8.350.2)] and lower incomplete gamma function [21, Eq. (8.350.1)] are represented by $\Gamma(\alpha) = \int_0^\infty t^{\alpha-1} e^{-t} dt$, $\Gamma(\alpha, x) = \int_x^\infty t^{\alpha-1} e^{-t} dt$ and $\gamma(\alpha, x) = \int_0^x t^{\alpha-1} e^{-t} dt$, respectively. $E_n(x) = \int_1^\infty (e^{-xt}/t^n) dt$ is the exponential integral function and $\mathcal{Y}_n(\cdot)$ is the second kind of Bessel function with order n . Finally, probability density function (PDF) and the cumulative distributed function (CDF) of random variable Z are illustrated as $f_Z(z)$ and $F_Z(z)$, respectively.

2 System and channel model

In this research, we consider a wireless cooperative communication system in which relaying selection is applied at the destination node and EH is implemented at the relay nodes. Furthermore, the source node S may communicate with the destination node D directly or via the best selected relay node in set of multiple relay nodes R_n with $n \in 1, \dots, N$ that forwards the received messages from the source node to the destination node as shown in Fig. 1.

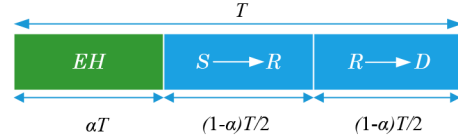


Fig. 2 TS protocol of a dual-hop relay system with EH scheme

The fundamental strategy to select the best relay node is that the source node chooses the best link from S to R corresponding to the maximum SNR in set of multi relay nodes. Mathematically, R_b is defined as [22]

$$R_b = \max_{n=1 \div N} \gamma_{SR_n}, \quad (1)$$

where γ_{SR_n} denotes the SNR of the link between S and R_n .

In the proposed system, there are three fading links between the source node and the destination node, the source node and the relay nodes, and the relay nodes and the destination node. Let the $|h_{SD}|^2$, $|h_{SR}|^2$ and $|h_{RD}|^2$ be amplitudes of these fading links, respectively. Without any loss of generality, in order to realise analysis, we assume that the amplitude of the fading channel is constant during each block time, but varies independently between blocks; the CSI is available at receiving nodes with a support of the added pilot signals, however, it is unavailable at transmitting nodes owing to none feedback communications.

The parameter m in the Nakagami- m distribution demonstrates the severity of fading and the smaller value of m informs more fading in the channel. Three Nakagami- m fading channels between $S-R$, $R-D$, $S-D$ are also represented by variable parameters (m_0, λ_0) , (m_1, λ_1) and (m_2, λ_2) , respectively. Where, the notation $\lambda_i = E\{Z\}$ is the mean of variable Z with $i \in \{0, 1, 2\}$ and $Z \subset \{|h_{SD}|^2, |h_{SR_b}|^2, |h_{R_bD}|^2\}$. Therefore, PDF and CDF of the variable Z can be considered as the Gamma distribution corresponding to the parameters $m_i > 0$ and $\lambda_i > 0$, expressed by following equations [4, 23]

$$f_Z(z) = \left(\frac{m_i}{\lambda_i}\right)^{m_i} \frac{z^{m_i-1}}{\Gamma(m_i)} \exp\left(-\frac{m_i z}{\lambda_i}\right), \quad (2)$$

$$F_Z(z) = \frac{1}{\Gamma(m_i)} \gamma\left(m_i, \frac{m_i z}{\lambda_i}\right). \quad (3)$$

3 EH model

In the considered system, while both the source and destination nodes are power supplied normally, the relay nodes are power supported by harvesting technique. Each relay node has only one antenna, operates in half duplex mode and contains an EH receiver and a data decode (ID) receiver with an assumption that they operate at the same frequency. Furthermore, in order to analyse both DF and AF protocols, the relay nodes are controlled on a high layer [24]. In this work, the TS [The power-splitting strategy can be utilised straightforwardly.] the strategy is applied at the relay nodes. [25]. Let the T denote the block time. The αT , $0 \leq \alpha \leq 1$, is a part of block time for the relay nodes harvesting energy from the around radio environment and the remained block time, $(1-\alpha)T$ is used for communication process in which the first half $(1-\alpha)T/2$ is time duration of receiving the signal from the source whereas the last half $(1-\alpha)T/2$ is time duration of forwarding the received signal to the destination (Fig. 2).

3.1 Linear EH model

In the conventional linear EH model, the value of energy harvested from the environment at the relay node, E_h , in the time duration αT can be computed as [26]

$$E_h = \frac{\eta P_S |h_{SR_b}|^2 \alpha T}{N_0}, \quad (4)$$

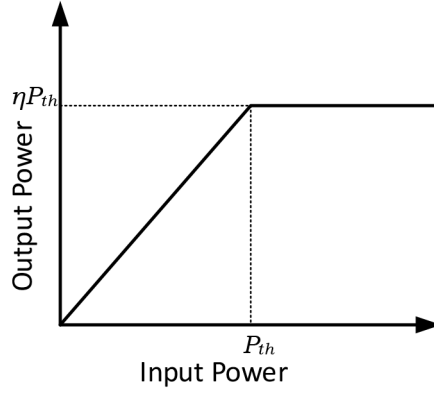


Fig. 3 Non-linear output

where P_S denotes the transmit power of the source node and $0 \leq \eta \leq 1$ expresses the energy conversion efficiency. This parameter basically relies on the rectification process and characteristics of the EH circuit. In this paper, the harvest-use protocol as in [27, 28] is utilised. The protocol indicates how to use energy in which the harvested energy in the EH phase is accumulated in a super-capacitor and then totally consumed to forward the source signal to the destination with an assumption that the power consumption of the circuit at the relay nodes can be considered as a negligible quantity. Thus the power of the best relay is given as

$$P_R = \frac{E_h}{(1-\alpha)T/2} = \frac{2\alpha\eta}{1-\alpha} P_S |h_{SR_b}|^2. \quad (5)$$

3.2 Non-linear EH model

In practice, the output power of energy harvesters frequently has saturation values that depend on the EH circuit parameters such as capacitors, inductors, diodes and etc. leading to non-linearly converting from the RF energy to the DC energy. The non-linear EH model can be demonstrated by a function that shows a relationship between the input RF power and the output DC power of the energy harvester as in Fig. 3. Here P_{th} is a saturation power threshold of the energy harvester. As a result, the transmission power of R is given as

$$P_R = \begin{cases} \frac{2\alpha\eta}{1-\alpha} P_S |h_{SR_b}|^2, & P_S |h_{SR_b}|^2 \leq P_{th} \\ \frac{2\alpha\eta}{1-\alpha} P_{th}, & P_S |h_{SR_b}|^2 > P_{th}. \end{cases} \quad (6)$$

4 Signal processing

In the first time slot of the signal processing phase, received signals at the relay nodes $y_R(t)$ and the destination node $y_D(t)$ during the broadcasting phase can be represented as [29]

$$y_R(t) = \sqrt{P_S} h_{SR} x(t) + n_R(t), \quad (7)$$

$$y_D(t) = \sqrt{P_S} h_{SD} x(t) + n_D(t), \quad (8)$$

where t expresses the symbol index and P_S denotes the transmit power of the source node. The sampled and normalised data signal from the source node is illustrated by $x(t)$. The additive white Gaussian noise with power spectral density N_0 at the relay and the destination nodes are represented by $n_R(t)$ and $n_D(t)$, respectively.

In the last half of communication phase, the best relay node R_b will re-code in case of the DF protocol or amplify in case of the AF protocol the received signal from the source node and then forward it to the destination node in $((1-\alpha)/2)T$ second. As a result, the received signal at the destination node in case of the DF protocol is given as

$$y_D(t) = \sqrt{P_R} h_{R_b D} \hat{x}(t) + n_D(t), \quad (9)$$

where $\hat{x}(t)$ denotes the signal decoded at the best relay node, P_R denotes the transmit power of the relay node, which depends on the harvesting model, i.e. linear/non-linear as in (5) and (6). And the received signal at the destination node in case of the AF protocol is given as [30]

$$y_D(t) = G h_{R_b D} y_R(t) + n_D(t), \quad (10)$$

where $G = \sqrt{P_R / (P_S |h_{SR_b}|^2 + \sigma_R^2)}$ denotes the amplification factor that is adjusted to remain the transmit power of the relay node [31].

Depending on (7), (8) and (10), the instantaneous SNR of each link can be determined. Let the γ_{AB} denote the instantaneous SNR of a link from the node A to the node B , with $A \in \{S, R_b\}$ and $B \in \{R_b, D\}$

$$\gamma_{SR_b} = \frac{P_S |h_{SR_b}|^2}{N_0}, \quad (11)$$

$$\gamma_{R_b D} = \frac{P_R}{N_0} |h_{R_b D}|^2, \quad (12)$$

$$\gamma_{SD} = \frac{P_S |h_{SD}|^2}{N_0}. \quad (13)$$

Regarding the end-to-end SNR γ_{e2e} , when the DF relay protocol is used, it is the minimum of γ_{SR_b} and $\gamma_{R_b D}$, i.e. [22]:

$$\gamma_{e2e} = \min(\gamma_{SR_b}, \gamma_{R_b D}). \quad (14)$$

When the AF protocol is used, the relay amplifies the received signals from the source node and then forwards them to the destination node. Hence, the end to end SNR, γ_{e2e} can be defined as [32, 33]

$$\gamma_{e2e} = \frac{\gamma_{SR_b} \gamma_{R_b D}}{\gamma_{SR_b} + \gamma_{R_b D} + 1}. \quad (15)$$

If the bandwidth is normalised, in each connecting scenario, the maximum average mutual information between the source node and destination node, in other words, the channel capacity can be calculated as

$$C_{SD} = \log_2(1 + \gamma_{SD}), \quad (16)$$

$$C_R = \frac{1-\alpha}{2} \log_2(1 + \gamma_{e2e}). \quad (17)$$

Here the pre-factor $(1-\alpha)/2$ is taken into account for communication between the source node and the destination node with support of the relay nodes.

5 Outage analysis

The OP is determined as the probability in a condition that the capacity of channel is lower than a defined transmission rate, $C < \mathcal{R}$. In fact, the OP plays a fundamental role in the evaluation and analysis of the system performance, consequently, it is used to clarify many wireless communication systems. The main aim of this section is to find out a closed-form expression for the OP. Based on the previous section, the OP can be determined logically as [1]

$$\begin{aligned} \text{OP} &= \Pr \left(\max \left\{ \log_2(1 + \gamma_{\text{SD}}), \frac{1-\alpha}{2} \log_2(1 + \gamma_{\text{e2e}}) \right\} < \mathcal{R} \right) \\ &= \Pr \left(\log_2(1 + \gamma_{\text{SD}}) < \mathcal{R}, \frac{1-\alpha}{2} \log_2(1 + \gamma_{\text{e2e}}) < \mathcal{R} \right). \end{aligned} \quad (18)$$

To solve the above equation, the CDF and PDF of the random variables are needed to compute, beginning with the following remark.

Remark 1: (Order Statistic): In the proposed model, the N relay nodes are utilised to forward received signals from the source node to the destination node. Let X_1, X_2, \dots, X_N denote the sequence of the independent random variables corresponding to the order statistic. A link which contains the largest instantaneous SNR can be selected and then assigned as the best relay, being demonstrated by the following criterion:

$$X = \max\{X_1, X_2, \dots, X_N\}. \quad (19)$$

The PDF of X is illustrated as follows:

$$f_X(x) = N f_{X_1}(x) [F_{X_1}(x)]^{N-1}. \quad (20)$$

Based on Remark 1, let us substitute (2) and (3) into (20) and after performing some modified operations, the PDF of X can be derived as

$$\begin{aligned} f_X(x) &= \left(\frac{m_1}{\lambda_1} \right)^{m_1} \frac{N x^{m_1-1}}{\Gamma(m_1)^N} \\ &\times \exp\left(-\frac{m_1 x}{\lambda_1}\right) \left[\gamma\left(m_1, \frac{m_1 x}{\lambda_1}\right) \right]^{N-1}. \end{aligned} \quad (21)$$

By employing [21, Eq. (8.352.4)], we have

$$\gamma(m, z) = \Gamma(m) \left[1 - e^{-z} \sum_{k=0}^{m-1} \frac{z^k}{k!} \right]. \quad (22)$$

Substituting (22) into (21) and utilising the Newton binomial expansion, (21) can be rewritten as

$$\begin{aligned} f_X(x) &= \sum_{n=0}^{N-1} \binom{N-1}{n} \frac{N x^{m_1-1} (-1)^n (m_1)^{m_1}}{\Gamma(m_1)^{N-1}} \left(\frac{m_1}{\lambda_1} \right)^{m_1} \\ &\times \exp\left(-\frac{m_1(n+1)x}{\lambda_1}\right) \left[\sum_{k=0}^{m_1-1} \frac{1}{k!} \left(\frac{m_1 x}{\lambda_1} \right)^k \right]^n. \end{aligned} \quad (23)$$

The inner sum in (23) is a polynomial of variable $z = m_1 x / \lambda_1$. The degree of this polynomial is $(m_1 - 1)$ and its coefficients are $a_k = 1/k!$.

The n th term of this polynomial is also a polynomial having a degree of $n(m_1 - 1)$ [34, Eq. (18)]

$$\left[\sum_{k=0}^{m_1-1} (a_k z^k) \right]^n = \sum_{k=0}^{n(m_1-1)} (b_k^n z^k). \quad (24)$$

Here the coefficient b_k^n can be recursively computed as [21, Eq. (0.314)]

$$b_0^n = 1, b_1^n = n, b_{n(m_1-1)}^n = \left(\frac{1}{(m_1-1)!} \right)^n, \quad (25a)$$

$$b_k^n = \frac{1}{k} \sum_{j=1}^{J_0} \frac{j(n+1)-k}{j!} b_{k-j}^n, \quad (25b)$$

$$J_0 = \min(k, m_1 - 1), \quad 2 \leq k \leq n(m_1 - 1) - 1. \quad (25c)$$

As mentioned in the Section 1, there have not been reports in any literature about performance evaluation of the cooperative communication system over Nakagami- m fading channels based on the OP expression with arbitrary m parameter. Moreover, to the best of the author's knowledge, our proposed cooperative communication system model that utilises dual-hop selection relay and EH technique under the existence of the direct link have not been analysed adequately in any published paper. As a result, we hope to develop and derive the closed-form expression of the OP with arbitrary m parameter in both cases of DF and AF protocol by following propositions.

5.1 DF protocol with EH

Proposition 1: The OP of the relaying network over Nakagami- m fading channel with an arbitrary m parameter which employs EH technique and the DF protocol can be demonstrated as

$$\text{OP}_{\text{DF}} = \frac{1}{\Gamma(m_0)} \gamma\left(m_0, \frac{m_0 \gamma_0}{\lambda_0 P_S}\right) \mathbb{J}(a, b). \quad (26)$$

where $\mathbb{J}(a, b)$ can be separated into two parts $\mathbb{J}(a, b) = \mathbb{J}_1 + \mathbb{J}_2$, expressed in two following equations:

$$\begin{aligned} \mathbb{J}_1 &= \sum_{k=0}^{\mathcal{N}_t} \frac{N c_k}{\Gamma(m_1)} \left(\frac{m_1}{\lambda_1} \right)^{N m_1} \left(\frac{N m_1}{\lambda_1} \right)^{-N m_1 - k} \\ &\times \Gamma\left(N m_1 + k, \frac{a N m_1}{\lambda_1}\right), \end{aligned} \quad (27)$$

and

$$\begin{aligned} \mathbb{J}_2 &= \sum_{k=0}^{\mathcal{N}_t} \sum_{j=0}^{\mathcal{N}_t} \sum_{t=0}^{\mathcal{N}_t} \frac{(-1)^t N c_k}{t! \Gamma(m_2 + j + 1)} \left(\frac{m_2 b}{\lambda_2} \right)^{m_2 + j + t} \\ &\times \left(\frac{m_1}{\lambda_1} \right)^{N m_1} \frac{1}{\Gamma(m_1)} \underbrace{\int_a^\infty x^v \exp\left(-\frac{N m_1 x}{\lambda_1}\right) dx}_{\Delta(x)}, \end{aligned} \quad (28)$$

here

$$\Delta(x) = \left(\frac{N m_1}{\lambda_1} \right)^{-v-1} \Gamma\left(v+1, \frac{a N m_1}{\lambda_1}\right), \quad \text{if } v \geq 0, \quad (29)$$

$$= \left(\frac{1}{a} \right)^{v-1} E_v\left(\frac{a N m_1}{\lambda_1}\right), \quad \text{if } v < 0, \quad (30)$$

with $v = N m_1 + k - m_2 - j - t - 1$.

The approximation of $\mathbb{J}(a, b)$ is provided as

$$\begin{aligned} \mathbb{J}(a, b) &\leq \sum_{k=0}^{\mathcal{N}_t} \sum_{j=0}^{\mathcal{N}_t} \frac{1}{\Gamma(m_1)} \left(\frac{m_1}{\lambda_1} \right)^{N m_1} \left(\frac{m_2 b}{\lambda_2} \right)^{m_2 + j} \\ &\times \frac{c_k N}{\Gamma(m_2 + j + 1)} 2 \left(\frac{m_2 b \lambda_1}{N m_1 \lambda_2} \right)^{(N m_1 + k - m_2 - j)/2} \\ &\times \mathcal{K}_{N m_1 + k - m_2 - j} \left(2 \sqrt{\frac{N m_1 m_2 b}{\lambda_1 \lambda_2}} \right), \end{aligned} \quad (31)$$

with $\mathcal{N}_t \in \{1; \infty\}$.

Proof: Since the direct link is independent of the forward link, we can substitute (11)–(13) into (18) to obtain the OP expression as

$$\text{OP} = \underbrace{\Pr(\gamma_{\text{SD}} < 2^{\mathcal{R}} - 1)}_{\mathcal{O}_1} \underbrace{\Pr(\min(\gamma_{\text{SR}_b}, \gamma_{\text{RD}}) < 2^{(2\mathcal{R}/(1-\alpha))} - 1)}_{\mathbb{J}(a,b)}. \quad (32)$$

It clear that the EH technique does not influence on received signals at the destination node via the direct link, consequently, the OP of the direct link can be expressed as:

$$\begin{aligned} \mathcal{O}_1 &= \Pr\left(\gamma_{\text{SD}} < \frac{\gamma_0 \sigma_{\text{D}}^2}{P_{\text{S}}}\right) \\ &= \frac{1}{\Gamma(m_0)} \gamma\left(m_0, \frac{m_0 \gamma_0 \sigma_{\text{D}}^2}{\lambda_0 P_{\text{S}}}\right), \end{aligned} \quad (33)$$

where $\gamma_0 = 2^{\mathcal{R}} - 1$. The term $\mathbb{J}(a,b)$ is illustrated later in Section 10.1 of the Appendix. \square

5.2 AF protocol with EH

Proposition 2: The OP of the relaying network over Nakagami- m fading channel with arbitrary m parameter which employs EH technique and the AF protocol can be demonstrated as

$$\text{OP} = \frac{1}{\Gamma(m_0)} \gamma\left(m_0, \frac{m_0 \gamma_0}{\lambda_0 P_{\text{S}}}\right) \mathbb{P}(x), \quad (34)$$

$$\mathbb{P}(x) = \sum_{k=0}^N \frac{Nc_k}{\Gamma(m_1)\Gamma(m_2)} \left(\frac{m_1}{\lambda_1}\right)^{Nm_1} (\mathbb{B}_1(x) - \mathbb{B}_2(x)), \quad (35)$$

$$\mathbb{B}_1(x) = \Gamma(m_2) \left(\frac{Nm_1}{\lambda_1}\right)^{-Nm_1-k} \Gamma\left(Nm_1+k, \frac{Nm_1 \gamma_{\text{th}}}{\lambda_1 P_{\text{S}}}\right), \quad (36)$$

and

$$\begin{aligned} \mathbb{B}_2(x) &= \sum_{j=0}^N \sum_{i=0}^{Nm_1+k-1} \binom{Nm_1+k-1}{i} \frac{\Gamma(m_2)(\phi \gamma_{\text{th}})^i}{\Gamma(m_2+j+1)\phi P_{\text{S}}} \\ &\times \exp\left(-\frac{Nm_1 \gamma_{\text{th}}}{\lambda_1 P_{\text{S}}}\right) \left(\frac{1}{\phi P_{\text{S}}}\right)^{Nm_1+k-1} \left(\frac{m_2 \gamma_{\text{th}}}{\lambda_2}\right)^{j+m_2} \\ &\times 2 \left(\frac{m_2 \gamma_{\text{th}} \lambda_1 \phi P_{\text{S}}}{\lambda_2 Nm_1}\right)^{\frac{v}{2}} \mathcal{K}_v\left(2\sqrt{\frac{Nm_1 m_2 \gamma_{\text{th}}}{\lambda_2 \lambda_1 \phi P_{\text{S}}}}\right). \end{aligned} \quad (37)$$

Proof: Based on the CDF of the SNR over the direct link and over the forward link and (15) and (18), the OP expression in case of AF protocol can be represented as

$$\begin{aligned} \text{OP}_{\text{AF}} &= \Pr(\gamma_{\text{SD}} < \gamma_0) \Pr\left(\frac{\gamma_{\text{SR}} \gamma_{\text{RD}}}{\gamma_{\text{SR}} + \gamma_{\text{RD}} + 1} < \gamma_{\text{th}}\right) \\ &\simeq \underbrace{\Pr(\gamma_{\text{SD}} < \gamma_0)}_{\mathcal{Q}_1(x)} \underbrace{\Pr\left(\frac{\gamma_{\text{SR}} \gamma_{\text{RD}}}{\gamma_{\text{SR}} + \gamma_{\text{RD}}} < \gamma_{\text{th}}\right)}_{\mathcal{Q}_2(x)}. \end{aligned} \quad (38)$$

here $\gamma_{\text{th}} = 2^{(2\mathcal{R}/(1-\alpha))} - 1$ and $\gamma_0 = 2^{\mathcal{R}} - 1$. The first part of the OP expression, $\mathcal{Q}_1(x)$, plays a role of the CDF of SNR over the direct link in which the communication channel from the source node to the destination node exists only in the first phase, therefore, it can be computed as in (33).

The second part of the probability, $\mathcal{Q}_2(x)$, can be represented as

$$\begin{aligned} \mathcal{Q}_2(x) &= \Pr\left(\frac{P_{\text{S}} |h_{1,i}|^2 \delta P_{\text{S}} |h_{1,i}|^2 |h_2|^2}{P_{\text{S}} |h_{1,i}|^2 + \delta P_{\text{S}} |h_{1,i}|^2 |h_2|^2} < \gamma_{\text{th}}\right) \\ &= \Pr\left(\frac{|h_{1,i}|^2 |h_2|^2}{1 + \delta |h_2|^2} < \frac{\gamma_{\text{th}}}{\delta P_{\text{S}}}\right), \end{aligned} \quad (39)$$

where $\delta = (2\alpha\eta)/(1-\alpha)$.

Once again, (39) can be represented as

$$\begin{aligned} \mathcal{Q}_2(x) &= \Pr\left(\frac{XY}{1+\delta Y} < \frac{\gamma_{\text{th}}}{\delta P_{\text{S}}}\right) \\ &= \int_0^{\gamma_{\text{th}}/P_{\text{S}}} \underbrace{\Pr\left(Y \geq \frac{\gamma_{\text{th}}}{\delta P_{\text{S}} x - \delta \gamma_{\text{th}}}\right)}_{=1} f_X(x) dx \\ &\quad + \int_{\gamma_{\text{th}}/P_{\text{S}}}^{\infty} \Pr\left(Y < \frac{\gamma_{\text{th}}}{\delta P_{\text{S}} x - \delta \gamma_{\text{th}}}\right) f_X(x) dx. \end{aligned} \quad (40)$$

Substituting (3) into (40) and after some algebraic manipulations, we can expand (40) as follows:

$$\begin{aligned} \mathcal{Q}_2(x) &= \int_0^{\gamma_{\text{th}}/P_{\text{S}}} f_X(x) dx \\ &\quad + \int_{\gamma_{\text{th}}/P_{\text{S}}}^{\infty} \left\{1 - \frac{1}{\Gamma(m_2)} \Gamma\left[m_2, \left(\frac{\beta_2 \gamma_{\text{th}}}{\delta P_{\text{S}} x - \delta \gamma_{\text{th}}}\right)\right]\right\} f_X(x) dx \\ &= \underbrace{\int_0^{\gamma_{\text{th}}/P_{\text{S}}} f_X(x) dx + \int_{\gamma_{\text{th}}/P_{\text{S}}}^{\infty} f_X(x) dx}_{=1} \\ &\quad - \int_{\gamma_{\text{th}}/P_{\text{S}}}^{\infty} \frac{1}{\Gamma(m_2)} \Gamma\left[m_2, \left(\frac{\beta_2 \gamma_{\text{th}}}{\delta P_{\text{S}} x - \delta \gamma_{\text{th}}}\right)\right] f_X(x) dx. \end{aligned} \quad (41)$$

As a result, we have

$$\mathcal{Q}_2(x) = 1 - \frac{1}{\Gamma(m_2)} \int_{\gamma_{\text{th}}/P_{\text{S}}}^{\infty} \Gamma\left[m_2, \left(\frac{\beta_2 \gamma_{\text{th}}}{\delta P_{\text{S}} x - \delta \gamma_{\text{th}}}\right)\right] f_X(x) dx, \quad (42)$$

where $\beta_2 = (m_2/\lambda_2)$. Substituting (52) into (42), the CDF over forward link is obtained as the following equation: (see (43)) Set the variable $u = \phi P_{\text{S}} x - \phi \gamma_{\text{th}}$ and execute binomial expansion, leading to the following equation:

$$\begin{aligned} \mathbb{B}_2(x) &= \sum_{j=0}^N \sum_{i=0}^{Nm_1+k-1} \binom{Nm_1+k-1}{i} \frac{\Gamma(m_2)(\phi \gamma_{\text{th}})^i}{\Gamma(m_2+j+1)} \\ &\times \exp\left(-\frac{Nm_1 \gamma_{\text{th}}}{\lambda_1 P_{\text{S}}}\right) \left(\frac{\beta_2 \gamma_{\text{th}}}{\phi P_{\text{S}}}\right)^{j+m_2} \left(\frac{1}{\phi P_{\text{S}}}\right)^{Nm_1+k-1} \\ &\times \int_0^{\infty} u^{Nm_1+k-i-j-m_2-1} \exp\left(-\frac{\beta_2 \gamma_{\text{th}}}{u} - \frac{Nm_1 u}{\lambda_1 \phi P_{\text{S}}}\right) du. \end{aligned} \quad (44)$$

Finally, based on the [21, Eq. (3.471.9)], we can find out $\mathbb{B}_2(x)$ as in (37). \square

$$\begin{aligned} F_{\text{YR}}(\gamma) &= 1 - \sum_{k=0}^N \frac{Nc_k}{\Gamma(m_1)\Gamma(m_2)} \left(\frac{m_1}{\lambda_1}\right)^{Nm_1} \\ &\times \underbrace{\int_{\gamma_{\text{th}}/P_{\text{S}}}^{\infty} \left[\Gamma(m_2) - \gamma\left(m_2, \frac{\beta_2 \gamma_{\text{th}}}{\phi P_{\text{S}} x - \phi \gamma_{\text{th}}}\right)\right] x^{Nm_1+k-1} \exp\left(-\frac{Nm_1 x}{\lambda_1}\right) dx}_{\mathbb{B}_1(x) - \mathbb{B}_2(x)}. \end{aligned} \quad (43)$$

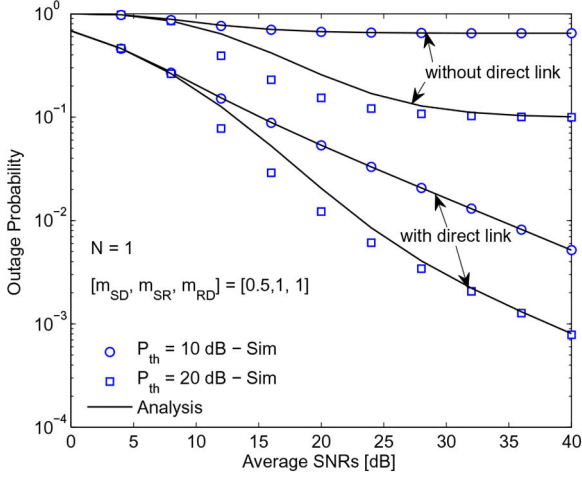


Fig. 4 Comparison between outage probabilities in case of the non-linear EH model and the DF protocol with and without the direct link versus average SNRs

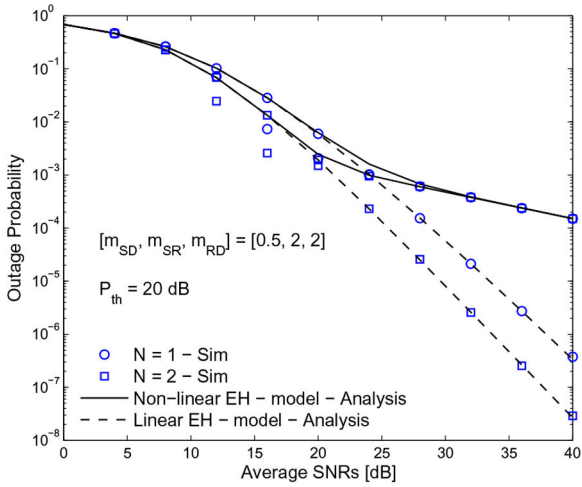


Fig. 5 Comparison between outage probabilities in cases of the linear and non-linear EH models versus average SNRs

5.3 OP with non-linear EH

In this subsection, the proposed system is analysed with the non-linear EH model, however, only the DF protocol is considered because similar results can be found out easily with the AF protocol. From (32), the OP expression can be rewritten as

$$OP = \mathcal{O}_1 \mathbb{J}(a, b), \quad (45)$$

where \mathcal{O}_1 is given in (33) and from the harvested energy given in (6), we have $\mathbb{J}(a, b)$ as

$$\mathbb{J}(a, b) = 1 - \underbrace{\Pr(\min(P_S X, \phi P_S X Y) > \gamma_{th}, P_S X \leq P_{th})}_{I_1} - \underbrace{\Pr(\min(P_S X, \phi P_{th} Y) > \gamma_{th}, P_S X > P_{th})}_{I_2}. \quad (46)$$

The following Lemma provides closed-form expressions of I_1 and I_2 to calculate the $\mathbb{J}(a, b)$.

Lemma 1: For the case of the non-linear EH model with DF protocol used at the relay nodes, $\mathbb{J}(a, b) = 1 - (I_1 + I_2)$, where I_1 and I_2 given as

$$I_1 = \sum_{k=0}^{\mathcal{N}_1} \sum_{j=0}^{m_2-1} \sum_{i=1}^M \frac{\pi}{j! M} \frac{N c_k}{\Gamma(m_i)} \left(\frac{m_i}{\lambda_1}\right)^{N m_i} \left(\frac{m_2 \gamma_{th}}{\lambda_2 \phi P_S}\right)^j \frac{P_{th} - \gamma_{th}}{2 P_S} \times u^{N m_1 + k - j - 1} \exp\left(-\frac{N m_1 u}{\lambda_1} - \frac{m_2 \gamma_{th}}{\lambda_2 \phi P_S u}\right) \sqrt{1 - \chi_i^2}, \quad (47)$$

where $\chi_i = \cos((2i-1)\pi/2M)$, $u = ((P_{th} - \gamma_{th})/2P_S)\chi_i + ((P_{th} + \gamma_{th})/2P_S)$, M is the number of terms, and π/M is the Gaussian weight.

$$I_2 = \begin{cases} \sum_{k=0}^{\mathcal{N}_1} \sum_{j=0}^{m_2-1} \frac{1}{j!} \frac{N c_k}{\Gamma(m_i)} \left(\frac{m_i}{\lambda_1}\right)^{N m_i} \left(\frac{m_2 \gamma_{th}}{\lambda_2 \phi P_{th}}\right)^j \exp\left(-\frac{m_2 \gamma_{th}}{\lambda_2 \phi P_{th}}\right) \times \left(\frac{\lambda_1}{N m_1}\right)^{N m_1 + k} \Gamma\left(N m_1 + k, \frac{N m_1 P_{th}}{\lambda_1 P_S}\right), & \text{if } P_{th} > \gamma_{th}, \\ \sum_{k=0}^{\mathcal{N}_1} \sum_{j=0}^{m_2-1} \frac{1}{j!} \frac{N c_k}{\Gamma(m_i)} \left(\frac{m_i}{\lambda_1}\right)^{N m_i} \left(\frac{m_2 \gamma_{th}}{\lambda_2 \phi P_{th}}\right)^j \exp\left(-\frac{m_2 \gamma_{th}}{\lambda_2 \phi P_{th}}\right) \times \left(\frac{\lambda_1}{N m_1}\right)^{N m_1 + k} \Gamma\left(N m_1 + k, \frac{N m_1 \gamma_{th}}{\lambda_1 P_S}\right), & \text{if } \gamma_{th} > P_{th}. \end{cases} \quad (48)$$

Proof: Based on the CDF and PDF of the SNR in case of DF protocol presented, the condition probability is used to derive I_1 and I_2 as given in Appendix. \square

6 Simulation results

In this section, numerical results are provided to verify the correctness of our theoretical analysis by Monte Carlo simulations with 2×10^{14} trials. Some main system parameters are assumed as follows. The Gaussian-Chebyshev parameter is chosen as $M = 50$. The number of terms in infinite series is a cut-off at $\mathcal{N}_1 = 25$. Noise components at all receiving nodes are assumed to have equal variance $\sigma^2 = 1$. The saturation power thresholds of energy harvester P_{th} are 10 and 20 dB. The best relay node is located at the middle of the source node and the destination node, therefore, the average channel gains are $E\{|h_{SR_b}|^2\} = \lambda_{1i} = 1$, $E\{|h_{R_bD}|^2\} = \lambda_{2j} = 1$ and $E\{|h_{SD}|^2\} = \lambda_0 = 2/3$. The data rate threshold is $\mathcal{R} = 1$ bit/s/Hz and the energy conversion efficiency factor of the converter is $\eta = 1$. The time ratio for EH is $\alpha = 0.3$. The number of relay nodes, $N \in \{1, 2, 3\}$, whereas the fading parameters, m , are selected by typical scenarios.

Fig. 4 illustrates the outage performance for the case of non-linear EH model and the DF protocol under a condition there is or is not the direct link. Without the direct link, the OPs decrease to saturated values in high SNR region. The reason is that the saturation power threshold of the energy harvester directly affects to the transmit power of the R , consequently, although SNR increases, the OPs do not decline in high SNR area. If the direct link appears, it contributes significantly to the system performance, therefore, the OPs also go down to saturated values but this process happens more slowly in comparison to the scenario of without the direct link. Moreover, in the case of $P_{th} = 20$ dB, the simulation results approximate to analysis results due to the approximation condition in the expressions (47) and (48).

In Fig. 5, the outage performance is evaluated and compared in cases of the linear and non-linear EH models in terms of different numbers of relay nodes. As can be seen from the figure, when SNR is < 20 dB, the outage probabilities of the linear EH model and non-linear EH model are the same. However, if SNR is > 20 dB, the OPs of the non-linear EH model are saturated, while the OPs of the linear EH model decrease continually as a function with respect to SNR. Since P_{th} is set at 20 dB, it limits the transmit power of the relay nodes as in (6). In addition, when the number of relay nodes increases, the outage performance in the case of the linear EH model is improved significantly. In contrast, the outage performance in case of the non-linear EH model does not depend on the number of relay nodes.

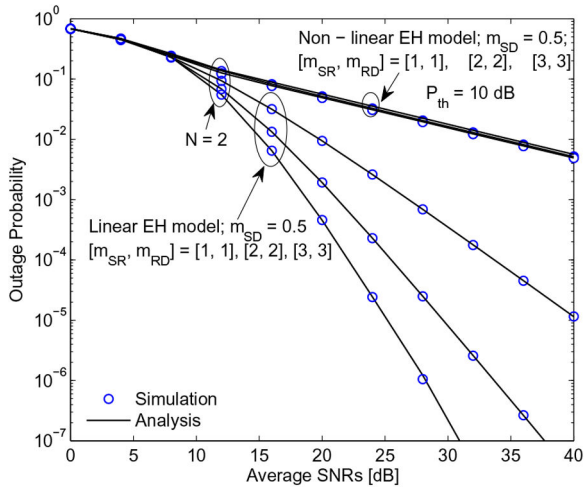


Fig. 6 Comparison between outage probabilities in cases of the linear/non-linear EH model versus average SNRs with different m

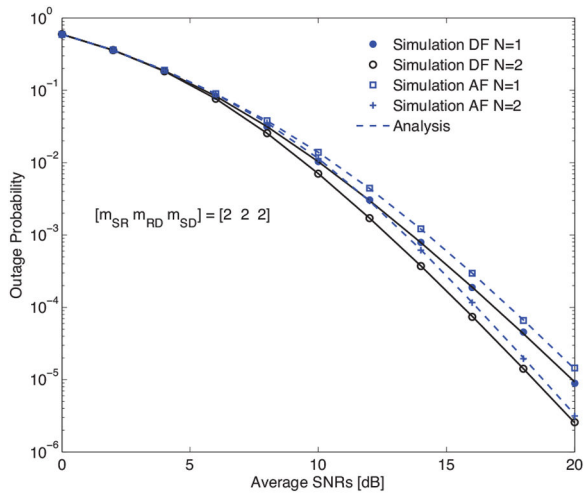


Fig. 7 Comparison between outage probabilities in cases of the AF and DF protocols versus average SNRs

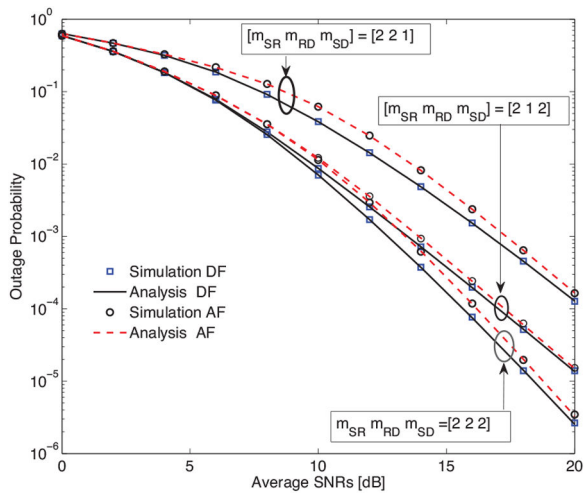


Fig. 8 OP in cases of different parameters m

In Fig. 6, the effect of m on the outage performance is illustrated.

It is clear that when m increases, the OPs of the linear EH model decrease significantly while the OPs of the non-linear EH model are likely to be independent of this parameter. In fact, in the linear EH model, if m as well as the number of lines of sight rises, the channel gain will improve due to an effective combination of received signals at the receiver. On the other hand, m affects slightly to the OPs of the non-linear EH model because the output

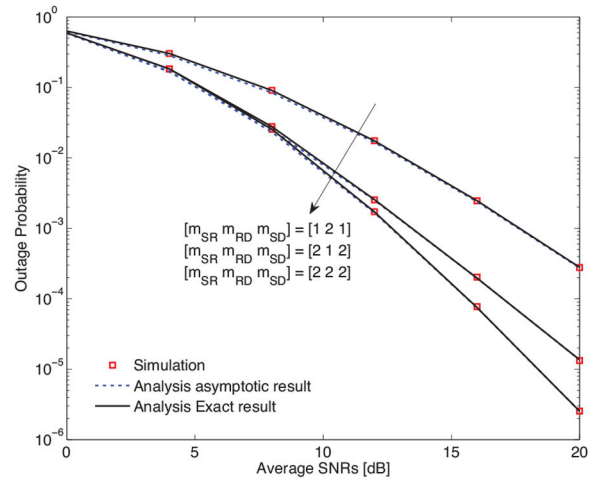


Fig. 9 Exact and approximate outage probabilities in cases of different parameters m

power of relay nodes is limited by P_{th} . Moreover, the OPs of the non-linear EH model are generally higher than the OPs of the linear EH model because the transmit power of relay nodes in case of the non-linear EH model is frequently lower than that of the linear EH model.

Fig. 7 presents the OP with respect to the average transmit power of the S . In this figure, the distribution parameter of the links S-R, R-D and S-D are set respectively as $[m_{SR}, m_{RD}, m_{SD}] = [2, 2, 2]$ for low complexity. As can be seen from Fig. 7, the DF protocol obtains slightly better performance than the AF protocol. Moreover, the perfect match between the mathematical analysis result and the Monte-Carlo simulation result in the case of integral m confirms the accuracy of the closed-form expression of OP. Therefore, the proposed analysis approach is precise and meaningful.

Fig. 8 illustrates the OP in cases of different parameters m , whereas other parameters are assumed to be the same as in Fig. 7. It is clear that if the parameter m increases, the OP decreases due to a reduction of fading. In addition, the OP in case of $[m_{SR}, m_{RD}] = [2, 2]$ is smaller than that of $[m_{SR}, m_{RD}] = [2, 1]$ because the fading of forward link depends on both links between S-R and R-D. Besides, the OP in case of $[m_{SD}] = [1]$ is higher than the OP in case of $[m_{SD}] = [2]$. The reason is that if the direct link quality is better than the forward link, the parameter m of the forward link does not influence on the system performance owing to the dependency of the SNR threshold for demodulation in the destination node on the SNR of the direct link. Moreover, small gaps between the outage probabilities based on the AF and DF protocols is illustrated and the excellent agreement between the simulation result and the analytical result is also demonstrated, confirming again the precision of the proposed analytical method.

Fig. 9 demonstrates the exact and approximate OP with an integral parameter m . This figure shows that the approximate OP is really close to the exact one and the trend is clearer in high SNR regions. As a result, the approximate OP expression can be used to evaluate the performance of the system in high SNR regions even for integral values of the fading severity parameters. The use of the approximate OP expression is more simple and effective while the accuracy is guaranteed.

Different from previous figures, Figs. 10 and 11 focus on the OP in case of arbitrary parameter m . As can be seen from Fig. 10, the gaps between the exact and approximate outage probabilities are absolutely small, especially in high SNR region. Obviously, the small gap between them comes from the approximate operation in (55), and the gap becomes smaller in high SNR region because the SNR is assumed to be high in this approximation. Moreover, if the number of the relay nodes increases as in Fig. 10 or m rises as in Fig. 11, the OP declines. This is explained as the system performance will be improved if there are more ways for transmitting signal from source to destination and the transmission environment becomes better. Finally, there is a great agreement between analysis and simulation in all scenarios.

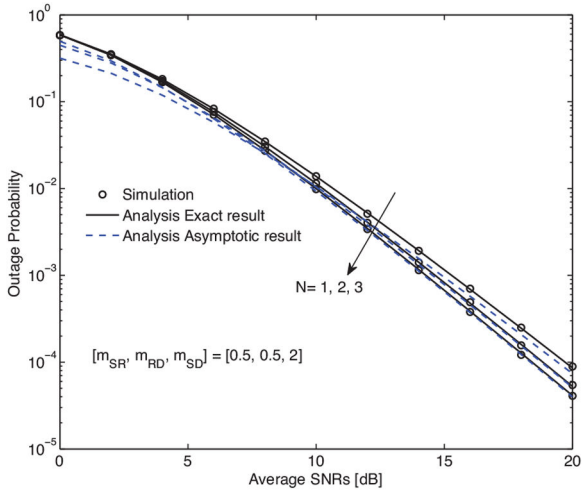


Fig. 10 Exact and approximate outage probabilities with different relay numbers and arbitrary m

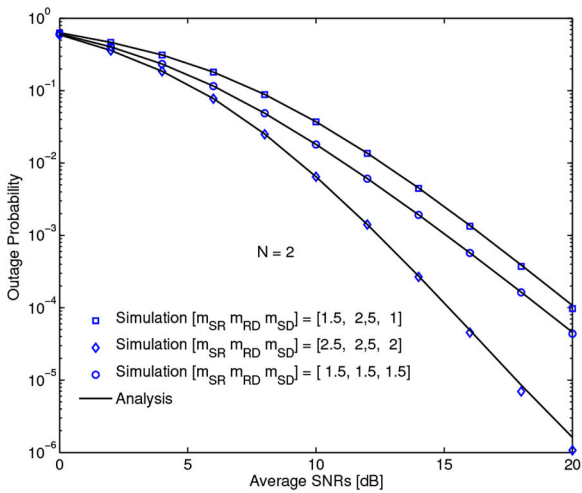


Fig. 11 OP with several parameters m

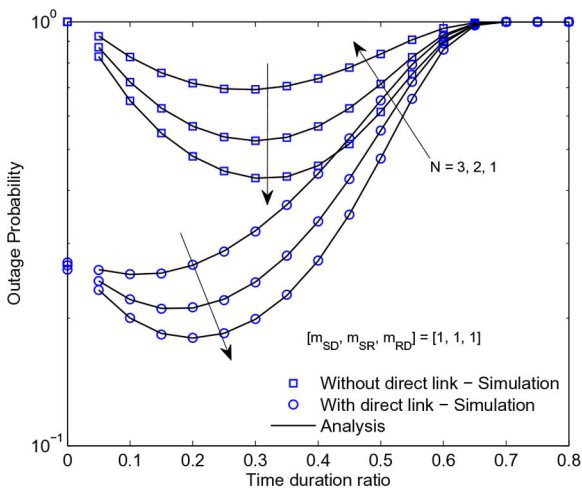


Fig. 12 OP versus EH ratio for different numbers of relay nodes, SNR = 5 dB

Fig. 12 presents the outage performance versus time duration of EH in two scenarios of with and without the direct link. In addition, the number of the relay nodes is varied while other parameters are fixed. As can be seen from the figure, the outage performance depends significantly on the time length of EH. Moreover, a system model having the direct link and more relay nodes may archive better outage performance than others.

7 Conclusions

In this work, the cooperative communication system over Nakagami- m fading channel applied EH technique was investigated. The system performance was evaluated by the OP. Different from previous works, the direct link, arbitrary m parameter, and both linear and non-linear EH models are taken into consideration. The approximate OP was also provided to improve analysis efficiency. The great agreement between mathematical analysis and Monte-Carlo simulation demonstrated the truth of the proposed method. In the future, the authors hope to analyse deeply the impact of the time duration for EH on the system performance and then optimise this parameter.

8 Acknowledgment

This research was funded by the Vietnam National Foundation for Science and Technology Development (NAFOSTED) under grant number 102.04-2017.311.

9 References

- [1] Laneman, J.N., Tse, D.N., Wornell, G.W.: 'Cooperative diversity in wireless networks: efficient protocols and outage behavior', *IEEE Trans. Inf. Theory*, 2004, **50**, (12), pp. 3062–3080
- [2] Bletsas, A., Shin, H., Win, M.Z.: 'Cooperative communications with outage-optimal opportunistic relaying', *IEEE Trans. Commun.*, 2007, **6**, (9), pp. 3450–3460
- [3] Duy, T.T., Duong, T.Q., Benevides, D., *et al.*: 'Proactive relay selection with joint impact of hardware impairment and co-channel interference', *IEEE Trans. Commun.*, 2015, **63**, (5), pp. 1594–1606
- [4] Duong, T.Q., Bao, V.N.Q., Zepernick, H.J.: 'On the performance of selection decode-and-forward relay networks over Nakagami- m fading channels', *IEEE Commun. Lett.*, 2009, **13**, (3), pp. 172–174
- [5] Lu, X., Wang, P., Niyato, D., *et al.*: 'Wireless networks with RF energy harvesting: a contemporary survey', *IEEE Commun. Tutor.*, 2015, **17**, (2), pp. 757–789
- [6] Zhao, L., Wang, X., Zheng, K.: 'Downlink hybrid information and energy transfer with Massive MIMO', *IEEE Commun. Mag.*, 2016, **15**, (2), pp. 1309–1322
- [7] Vahidnia, R., Anpalagan, A., Mirzaei, J.: 'Diversity combining in bi-directional relay networks with energy harvesting nodes', *IET Commun.*, 2016, **10**, (2), pp. 207–211
- [8] Do, N.T., Bao, V.N.Q., An, B.: 'A relay selection protocol for wireless energy relaying relay networks'. Proc. 12th Advanced Technologies Communications (ATC), Ho Chi Minh, Vietnam, October 2015, vol. 10, no. 2, pp. 243–247
- [9] Son, P.N., Kong, H.Y., Anpalagan, A.: 'Exact outage analysis of a decode-and-forward cooperative communication network with n th best energy harvesting relay selection', *Ann. Telecommun.*, 2016, **71**, (5–6), pp. 251–263
- [10] Chen, Y.: 'Energy-harvesting AF relaying in the presence of interference and Nakagami-Fading', *IEEE Trans. Commun.*, 2016, **15**, (2), pp. 1008–1017
- [11] Boshkovska, E., Zlatanov, N., Schober, R., *et al.*: 'Practical non-linear energy harvesting model and resource allocation for swipt systems', *IEEE Commun. Lett.*, 2015, **19**, (12), pp. 2082–2085
- [12] Chen, Y., Sabnis, K.T., Abd-Elhameed, R.A.: 'New formula for conversion efficiency of RF EH and its wireless applications', *IEEE Trans. Veh. Technol.*, 2016, **65**, (11), pp. 9410–9414
- [13] Xu, X., McKelvey, T., Viberg, M., *et al.*: 'Simultaneous information and power transfer under a non-linear RF energy harvesting model'. Proc. IEEE Int. Conf. Communications Workshops (ICC Workshops), Paris, France, July 2017, pp. 179–184
- [14] Clerckx, B., Zhang, R., Schober, R., *et al.*: 'Fundamentals of wireless information and power transfer: from RF energy harvester models to signal and system designs', *IEEE J. Sel. Areas Commun.*, 2019, **37**, (1), pp. 4–33
- [15] Xiong, K., Wang, B., Liu, K.R.: 'Rate-energy region of swipt for MIMO broadcasting under nonlinear energy harvesting model', *IEEE Trans. Wirel. Commun.*, 2017, **16**, (8), pp. 5147–5161
- [16] Dong, Y., Hossain, M., Cheng, J.: 'Performance of wireless powered amplify and forward relaying over Nakagami- m fading channels with nonlinear energy harvester', *IEEE Commun. Lett.*, 2016, **20**, (4), pp. 672–675
- [17] Hoang, T.M., Duy, T.T., Bao, V.N.Q.: 'On the performance of non-linear wirelessly powered partial relay selection networks over Rayleigh fading channels'. Proc. 3rd National Found Science and Technology Development Conf. (NICS), Danang, Vietnam, September 2016, vol. 10, no. 2, pp. 6–11
- [18] Hoang, T.M., Tan, N.T., Hiep, P.T., *et al.*: 'Performance analysis of decode-and-forward partial relay selection in NOMA systems with RF energy harvesting', *Wirel. Netw.*, 2019, **25**, pp. 4585–4595. Available at <https://doi.org/10.1007/s11276-018-1746-8>
- [19] Hoang, T.M., Son, V.V., Hiep, P.T., *et al.*: 'Optimizing duration of energy harvesting for downlink NOMA full-duplex over Nakagami- m fading channel', *Int. J. Electron. Commun.*, 2018, **95**, pp. 199–206
- [20] Hoang, T.M., Tan, N.T., Cao, N.B., *et al.*: 'Outage probability of MIMO relaying full-duplex system with wireless information and power transfer'. Proc. Conf. Information Communication Technology (CICT), Gwalior, India, November 2017, pp. 1–6

- [21] Zwillinger, D.: 'Table of integrals, series, and products' (Elsevier Press, Holland, 2014, 1st edn.)
- [22] Amin, O., Mesleh, R., Ikki, S.S., *et al.*: 'Performance analysis of multiple-relay cooperative systems with signal space diversity', *IEEE Trans. Veh. Technol.*, 2014, **64**, (8), pp. 3414–3425
- [23] Senaratne, D., Tellambura, C.: 'Unified exact performance analysis of two-hop amplify-and-forward relaying in Nakagami m fading', *IEEE Trans. Veh. Technol.*, 2010, **59**, (3), pp. 1529–1534
- [24] Bao, V.N.Q., Kong, H.Y.: 'Performance analysis of decode-and-forward relaying with partial relay selection for multihop transmission over Rayleigh fading channels', *J. Commun. Netw.*, 2010, **12**, (5), pp. 433–441
- [25] Nasir, A.A., Zhou, X., Durrani, S., *et al.*: 'Relaying protocols for wireless energy harvesting and information processing', *IEEE Trans. Wirel. Commun.*, 2013, **12**, (7), pp. 3622–3636
- [26] Krikidis, I., Timotheou, S., Sasaki, S.: 'RF energy transfer for cooperative networks: data relaying or energy harvesting', *IEEE Commun. Lett.*, 2012, **16**, (11), pp. 1772–1775
- [27] Sudevalayam, S., Kulkarni, P.: 'Energy harvesting sensor nodes: survey and implications', *IEEE Commun. Surv. Tutor.*, 2011, **13**, (3), pp. 443–461
- [28] Krikidis, I., Zheng, G., Ottersten, B.: 'Harvest-use cooperative networks with half/full-duplex relaying'. Proc. Wireless Communications and Networking Conf. (WCNC), Shanghai, China, April 2013, pp. 4256–4260
- [29] Stauffer, E., Oyman, O., Narasimhan, R., *et al.*: 'Finite-SNR diversity-multiplexing tradeoffs in fading relay channels', *IEEE J. Sel. Areas Commun.*, 2007, **25**, (2), pp. 245–257
- [30] Hu, W.W., Huang, W.J., Li, C.P., *et al.*: 'Lifetime maximization in AF cooperative networks with energy-harvesting relays'. Proc. IEEE Int. Symp. Broadband Multimedia Systems Broadcasting (BMSB), Cagliari, Italy, June 2017, pp. 1–4
- [31] Suraweera, H.A., Smith, P.J., Nallanathan, A., *et al.*: 'Amplify-and-forward relaying with optimal and suboptimal transmit antenna selection', *IEEE Trans. Wirel. Commun.*, 2011, **10**, (6), pp. 1874–1885
- [32] Krikidis, I., Thompson, J., McLaughlin, S., *et al.*: 'Amplify-and-forward with partial relay selection', *IEEE Commun. Lett.*, 2008, **12**, (4), pp. 235–237
- [33] Duy, T.T., Kong, H.-Y.: 'Performance analysis of hybrid decode-amplify-forward incremental relaying cooperative diversity protocol using SNR-based relay selection', *IEEE Commun. Lett.*, 2012, **14**, (6), pp. 703–709
- [34] Fedele, G.: 'N-branch diversity reception of many DPSK signals in slow and non selective Nakagami m fading', *IEEE Trans. Commun. Technol.*, 1996, **7**, (2), pp. 119–123
- [35] Hung, C.-C., Chiang, C.-T., Yen, N.-Y., *et al.*: 'Outage probability of multiuser transmit antenna selection/maximal-ratio combining systems over arbitrary Nakagami-m fading channels', *IET Commun.*, 2010, **4**, (1), pp. 63–68
- [36] Abramowitz, M., Stegun, I.A.: 'Handbook of mathematical functions: with formulas, graphs, and mathematical tables', vol. **55** (Courier Corporation Press, USA., 1964)

10 Appendix

10.1 Appendix: The proof of term $\mathbb{J}(a, b)$

By combining (11), (12) and (14), the function $\mathbb{J}(a, b)$ can be represented as

$$\begin{aligned} \mathbb{J}(a, b) &= 1 - \Pr(\gamma_{SR} > \gamma_{th}, \gamma_{RD} > \gamma_{th}) \\ &= 1 - \Pr(X > a, XY > b), \end{aligned} \quad (49)$$

where $\gamma_{th} = 2^{(2\mathcal{R}/(1-\alpha))} - 1$; $a = (\gamma_{th}/P_S)$, and $b = (1-\alpha)\gamma_{th}/2\alpha\eta P_S$.

The expansion of the incomplete Gamma function by a series development is applied for $\gamma(m, z)$ [35, Eq. (5)].

$$\gamma(m, z) = e^{-z} \sum_{k=0}^{\infty} \frac{\Gamma(m) z^{m+k}}{\Gamma(m+k+1)}. \quad (50)$$

From (50), it is clear that in case the Nakagami- m fading parameter is not integral, the CDF can be expressed as a single infinity series of incomplete Gamma function.

Substituting (50) into (21) and after some algebraic manipulations, the PDF of the instantaneous SNR over the first hop is obtained

$$\begin{aligned} f_X(x) &= \left(\frac{m_1}{\lambda_1}\right)^{Nm_1} \frac{N x^{Nm_1-1}}{\Gamma(m_1)} \exp\left(-\frac{Nm_1 x}{\lambda_1}\right) \\ &\times \left[\sum_{k=0}^{\infty} \left(\frac{m_1}{\lambda_1}\right)^k \frac{x^k}{\Gamma(m_1+k+1)} \right]^{N-1}. \end{aligned} \quad (51)$$

Based on [21, Eq. (0.314)], (51) can be represented as

$$f_X(x) = \sum_{k=0}^{\infty} c_k \left(\frac{m_1}{\lambda_1}\right)^{Nm_1} \frac{N x^{Nm_1+k-1}}{\Gamma(m_1)} \exp\left(-\frac{Nm_1 x}{\lambda_1}\right), \quad (52)$$

where c_k is denoted as

$$c_0 = \left[\frac{1}{\Gamma(m_1+1)} \right]^{N-1}, \quad \text{for } k=0, \quad (53a)$$

$$c_k = \sum_{\ell=1}^k \frac{\Gamma(m_1+1)}{k} \left(\frac{m_1}{\lambda_1}\right)^{\ell} \frac{(\ell N - k) c_{k-\ell}}{\Gamma(m_1+\ell+1)}, \quad \text{for } k \geq 1. \quad (53b)$$

Since the CDF and PDF of the individual link had been obtained by (3) and (52), the CDF of the link S-R-D can be derived as

$$\begin{aligned} \mathbb{J}(a, b) &= 1 - \int_a^{\infty} \left[1 - F_Y\left(\frac{b}{x}\right) \right] f_X(x) dx \\ &= 1 - \left[\int_a^{\infty} f_X(x) dx - \int_a^{\infty} F_Y\left(\frac{b}{x}\right) f_X(x) dx \right], \end{aligned} \quad (54)$$

where $b = ((1-\alpha)\gamma_{th}/2\alpha\eta P_S)$ and $a = (\gamma_{th}/P_S)$.

If the transmit power is high, the parameter a can be approximated as $a = (\gamma_{th}/(P_S \rightarrow \infty)) \approx 0$. Consequently, the $\mathbb{J}(a, b)$ is changed.

$$\begin{aligned} \mathbb{J}(a, b) &\leq \sum_{k=0}^{N_1} \sum_{j=0}^{N_1} \left(\frac{m_1}{\lambda_1}\right)^{Nm_1} \left(\frac{m_2 b}{\lambda_2}\right)^{m_2+j} \frac{c_k}{\Gamma(m_2+j+1)} \\ &\times \frac{N}{\Gamma(m_1)} \int_0^{\infty} x^v \exp\left(-\frac{m_2 b}{\lambda_2 x} - \frac{Nm_1 x}{\lambda_1}\right) dx. \end{aligned} \quad (55)$$

with $v = Nm_1 + k - m_2 - j - 1$.

Applying [21, Eq. (3.471.9)], we have

$$\begin{aligned} &\int_0^{\infty} x^v \exp\left(-\frac{m_2 b}{\lambda_2 x} - \frac{Nm_1 x}{\lambda_1}\right) dx \\ &= 2 \left(\frac{m_2 b \lambda_1}{Nm_1 \lambda_2}\right)^{(Nm_1+k-m_2-j)/2} \mathcal{K}_{Nm_1+k-m_2-j} \left(2\sqrt{\frac{Nm_1 m_2 b}{\lambda_1 \lambda_2}}\right), \end{aligned} \quad (56)$$

and then the approximation of $\mathbb{J}(a, b)$ in (55) is changed as in (31).

In order to evaluated exactly the OP, (3) and (52) are substituted into (54), and the function $\mathbb{J}(a, b)$ is computed as

$$\begin{aligned} \mathbb{J}(a, b) &= 1 - \underbrace{\sum_{k=0}^{\infty} \left(\frac{m_1}{\lambda_1}\right)^{Nm_1} \frac{c_k N}{\Gamma(m_1)} \int_a^{\infty} x^{Nm_1+k-1} \exp\left(-\frac{Nm_1 x}{\lambda_1}\right) dx}_{\mathbb{J}_1} \\ &+ \underbrace{\sum_{k=0}^{\infty} \left(\frac{m_1}{\lambda_1}\right)^{Nm_1} \frac{N c_k}{\Gamma(m_1)} \int_a^{\infty} F_Y\left(\frac{b}{x}\right) x^{Nm_1+k-1} \exp\left(-\frac{Nm_1 x}{\lambda_1}\right) dx}_{\mathbb{J}_2} \end{aligned} \quad (57)$$

To calculate the \mathbb{J}_1 , [21, Eq. (3.351.2)] can be used, while the variable x is changed as $x = au$ to calculate \mathbb{J}_2 and then (28) is obtained. In short, the system model is considered in two cases of index power $v \geq 0$ and $v < 0$. For detail, [21, Eq. (3.351.2)] is used in the case of $v \geq 0$ and the exponential integral function is used in the case of $v < 0$. As a result, Proposition 1 is completely proved.

10.2 Appendix: The proof for Lemma 1

From (46), I_1 is represented as

$$I_1 = \int_{a_2}^{a_1} \left[1 - F_Y\left(\frac{\gamma_{th}}{P_S \phi x}\right) \right] f_X(x) dx, \quad (58)$$

where $a_1 = P_{th}/P_S$ and $a_2 = \gamma_{th}/P_S$. Replacing $f_X(x)$ and $F_Y(y)$ from (3) and (52), we have I_1 as

$$I_1 = \sum_{k=0}^{\infty} \sum_{j=0}^{m_2-1} \left(\frac{m_1}{\lambda_1}\right)^{Nm_1} \frac{c_k N}{\Gamma(m_1)} \left(\frac{m_2 \gamma_{th}}{\lambda_2 \phi P_S}\right)^j \times \int_{a_2}^{a_1} x^{Nm_1+k-j-1} \exp\left(-\frac{Nm_1 x}{\lambda_1} - \frac{m_2 \gamma_{th}}{\lambda_2 \phi P_S x}\right) dx. \quad (59)$$

It is very difficult to exactly calculate the closed-form expression in (59). Based on Gaussian–Chebyshev quadrature in [36, Eq. (25.40)], we obtain an approximation of I_1 .

Besides, I_2 is calculated as

$$I_2 = \Pr(P_S X > \gamma_{th}, \phi P_{th} Y > \gamma_{th}, P_S X > P_{th}) \quad (60)$$

$$= \begin{cases} \int_{\gamma_{th}/P_S}^{\infty} \left[1 - F_Y\left(\frac{\gamma_{th}}{\phi P_{th}}\right)\right] f_X(x) dx, & \gamma_{th} > P_{th}, \\ \int_{P_{th}/P_S}^{\infty} \left[1 - F_Y\left(\frac{\gamma_{th}}{\phi P_{th}}\right)\right] f_X(x) dx, & P_{th} > \gamma_{th}. \end{cases} \quad (61)$$

By replacing $f_X(x)$ and $F_Y(y)$ from (3) and (52), and thank to the help of [21, Eq. (3.381.3)], we obtained I_2 after some manipulations.